

# ICRF HEATING, PARTICLE TRANSPORT AND FLUCTUATIONS IN TOKAMAKS\*

R.J. TAYLOR, P. LEE, N.C. LUHMANN, Jr.,  
A. MASE, G.J. MORALES, W.A. PEEBLES, A. SEMET,  
F. SCHWIRZKE, S. TALMADGE, S.J. ZWEBEN  
University of California at Los Angeles,  
Los Angeles, California

M.A. HEDEMANN, B.S. LEVINE, R.W. GOULD  
California Institute of Technology,  
Pasadena, California,  
United States of America

## Abstract

### ICRF HEATING, PARTICLE TRANSPORT AND FLUCTUATIONS IN TOKAMAKS.

The paper consists of three parts. Part A reports the results of ICRF heating at power levels up to five times Ohmic heating. The ions were heated from 50 to 200 eV while the electron temperature increased from 150 to 250 eV under optimum conditions. Impurity generation is controlled by Ti or Cr in-situ vapour deposition of about 100 Å thick. Heating is observed to vanish as the plasma density is raised above  $10^{13}$  cm<sup>-3</sup> in Macrotor and  $10^{14}$  cm<sup>-3</sup> in Microtor. Below these densities and at high power levels, the plasma particle confinement time, and consequently the energy confinement, diminishes with power input. Density clamping, drop or rise are produced depending on wall conditions. Part B describes magnetic field fluctuation measurements on the Caltech research tokamak. At low frequencies,  $f < 100$  kHz, the  $\tilde{B}$  spectrum is dominated by an  $m = 2$  or 3 mode and its harmonics, while at high frequencies,  $100 \text{ kHz} < f < 1 \text{ MHz}$ , the  $\tilde{B}$  fluctuations are broadband and have short correlation lengths. Part C reports on FIR scattering measurements of density fluctuations in the Microtor tokamak. The fluctuations exhibit a power law falloff of  $\omega^{-2.5}$  between 100 kHz and 500 kHz and  $k^{-3.5}$  for  $6 \text{ cm}^{-1} \lesssim k \lesssim 20 \text{ cm}^{-1}$ . A comparison of these measurements with theoretical models and with transport is presented.

## Part A

### HEATING AND TRANSPORT

*(R.J. Taylor, G.J. Morales, F. Schwirzke, S. Talmadge, S.J. Zweben)*

#### 1. INTRODUCTION

We have conducted an investigation into the nature of ICRF heating under a broad range of conditions using the Microtor and Macrotor tokamaks. The machine operating parameters are:

\* Supported by US Department of Energy Grant No. DE-AM03-76SF-00010.

Macrotor

$$0.1 \text{ T} < B_T < 0.4 \text{ T}$$

$$20 \text{ kA} < I_p < 100 \text{ kA}$$

$$1 \times 10^{12} \text{ cm}^{-3} < N_e < 3 \times 10^{13} \text{ cm}^{-3}$$

$$R = 0.9 \text{ m}; a = 0.4 \text{ m}$$

Microtor

$$1 \text{ T} < B_T < 2.5 \text{ T}$$

$$20 \text{ kA} < I_p < 120 \text{ kA}$$

$$1 \times 10^{13} \text{ cm}^{-3} < N_e < 5 \times 10^{14} \text{ cm}^{-3}$$

$$R = 0.3 \text{ m}; a = 0.1 \text{ m}$$

These devices obey the Alcator-A scaling law[1]. Particularly large flexibility is found in programming the density (beta) while keeping the temperature constant. This is attributed to the wall conditions and the low impurity levels. For example, the total impurity radiated power (edge plus center) can be kept below 1% of the ohmic input. The majority of the input power is lost by charged particle transport. The plasmas are often doped with CO<sub>2</sub> in order to increase the line radiation for diagnostic reasons. This gas is mixed into the working gas and puffed during the pulse.

RF power, up to 0.5 MW at  $0.5 \Omega_{CD} < \omega_{RF} < 6 \times \Omega_{CD}$ , is applied through loop couplers (antennae) located on the outside of the plasma. These may act as limiters when the plasma approaches them. We have investigated many different but simple antennae similar to the TFR designs[2], with and without shielding the currents and fields. Fig. 1 shows the placement of the antenna in a typical configuration.

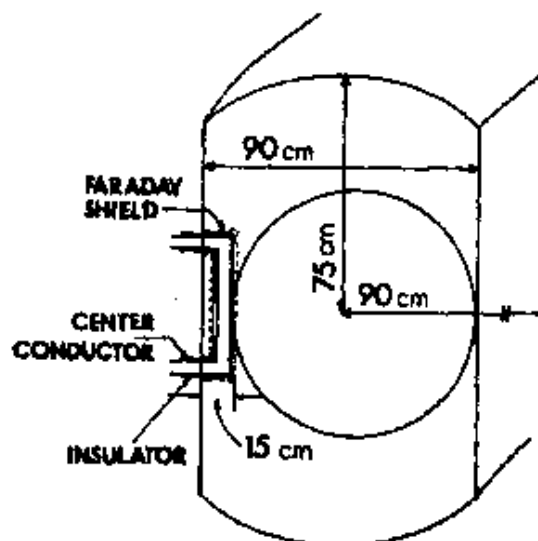


FIG.1. Placement of an antenna in Macrotor showing insulation of Faraday shielding. Improved coupling can be obtained by contouring the antenna to the plasma.

Two important ingredients have been found relating to antenna design: (1) avoid plasma current flowing to energized parts; and (2) place the loop close to the plasma edge. Electric fields (less than 10 kV/cm) around the insulators exposed to the plasma are found inconsequential, being shielded out by the plasma. However, on occasion we have used a Faraday shield to protect the insulators from sputtering, as shown in Fig. 1.

## 2. WAVE PROPAGATION

Fig. 2 shows the calculated propagation zone of the fast Alfvén wave in Macrotor, for various azimuthal mode numbers,  $n_\phi$ , in a deuterium plasma at the second harmonic. Here we followed

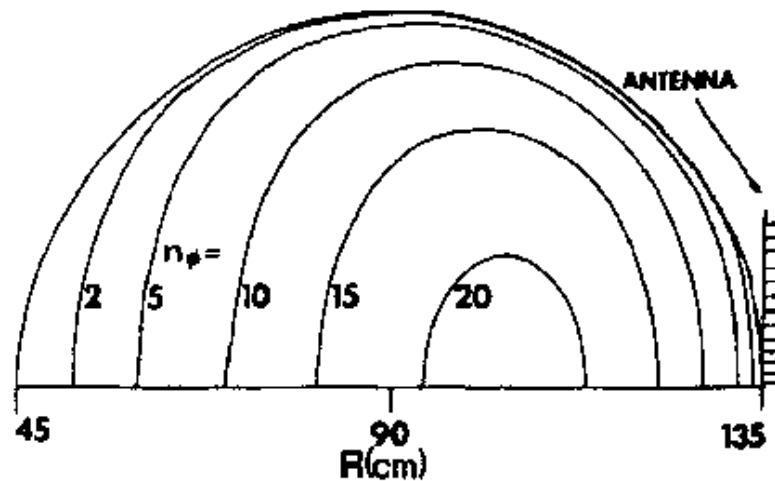


FIG.2. Calculated fast Alfvén wave propagation zones in Macrotron at  $n_c = 3 \times 10^{13} \text{ cm}^{-3}$ ,  $B_T = 3 \text{ kG}$  and  $\omega_{RF} = 2 \times \Omega_{CD}$  as a function of azimuthal mode numbers. The evanescent region increases with mode number.

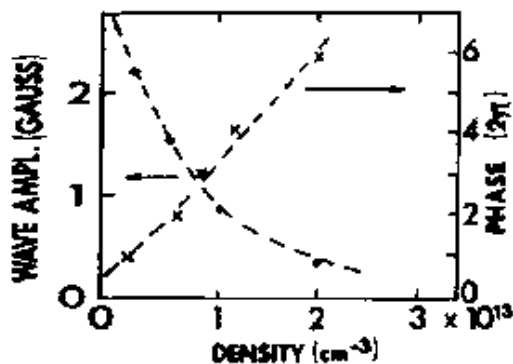


FIG.3. The measured ICRF wave amplitude and phase in Macrotron as a function of density. The azimuthal mode number is proportional to the phase. Similar results have been found in Microtron.

Perkins' formulation[3]. Due to the high density in these devices, large mode numbers can be propagated, up to  $n_\phi \sim 25$  in Macrotron at  $3 \times 10^{13} \text{ cm}^{-3}$  and 20 in Microtron at  $3 \times 10^{14} \text{ cm}^{-3}$  (not shown). Experimentally we find that the dominant  $k_{||}$  is selected by the plasma so that the mode number is approximately proportional to the density. Consequently, at high densities  $k_{||}$  is large and the propagating region narrows. The evanescent region between the antenna and the Alfvén cutoff layer therefore becomes wider. The consequence of this is seen in Fig. 3, where the dominant wave amplitude as received by a probe decreases while the wave number (phase) increases. Thus, the optimum heating is observed at moderate densities, about three times smaller than the maximum attainable in each device. This corresponds to a beta on axis of 1%.

### 3. ICRF HEATING

The heating has been investigated for a variety of conditions, the most promising being the ion-hybrid and the minority regimes,  $0.04 n_H/n_D < 0.5$ . Significant edge heating, ( $T_{RF} \sim 3 \times T_{OH}$ ) has been seen under most conditions, e.g. at the sixth harmonic of deuterium. Fig. 4 shows the time-dependence of the observed heating, in the two-ion regime. The ion heating was monitored by Doppler broadening of CV at the center. Figure 5 shows the typical spectrum of charge-exchange neutrals. Fast ions up to 10 keV can be produced in Macrotron. These ions are mainly lost by charge exchange on a 1-msec time scale, while the bulk ion confinement time is 5 msec.

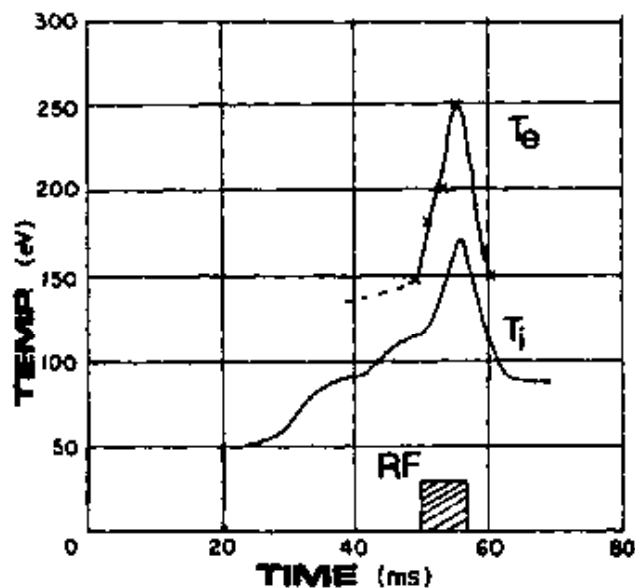


FIG. 4. Evolution of temperature during rf heating in the two-ion regime;  $n_H/n_D \approx 6\%$ .

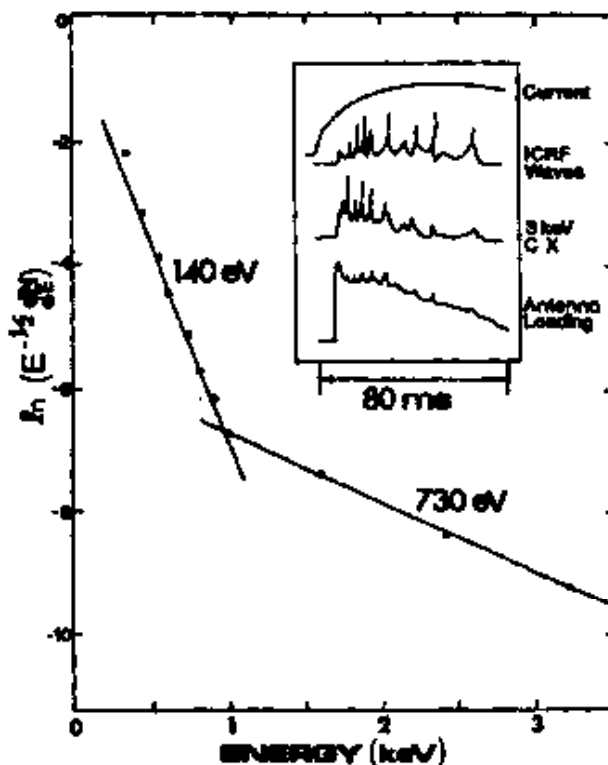


FIG. 5. Charge exchange  $T_i$  in the minority mode. The  $T_i$  without rf heating is 70 eV (not shown). The insert shows increased charge-exchange activity, loading and ICRF wave phenomena at the toroidal resonances.

In our experiments the ion temperature rises linearly with input power when the power is low. But when the RF power exceeds the ohmic heating power, the heating efficiency falls off due to a reduction of the particle confinement time. The heating saturates and the main effect of the additional heating power is to reduce the confinement. In Macrotor, therefore, we have realized conditions where an upper limit to power input is seen in terms of transport and not impurities or power transfer. In Microtor, the experiments have been limited to low power input due to the compactness of the device. More elaborate antenna designs are under investigation to increase the coupling without reducing plasma size. Even so, we were able to see enhanced charge-exchange flux activity at toroidal resonances. The heating efficiency in Microtor also decreases with density faster than  $1/n_e$ .

#### 4. TRANSPORT

The effect of the RF on the particle containment was not evaluated in earlier tokamak experiments. Generally, a density increase has been seen [4], possibly due to impurity influx. In Macrotor we have seen both density increases and decreases, depending on wall conditions. When the recycling rate is less than unity, as when the walls are clean and gas is puffed during the discharge, the density is observed to fall. This can result in the reduction of  $\tau_p$  to 1 msec from the usual 5 msec.

Fig. 6 shows this effect versus antenna current. The rate of fall has been extracted from the traces shown in the inset. The transport is observed to increase linearly with antenna current, in analogy with results from earlier experiments on other devices[5]. A mass dependence has also been noted.

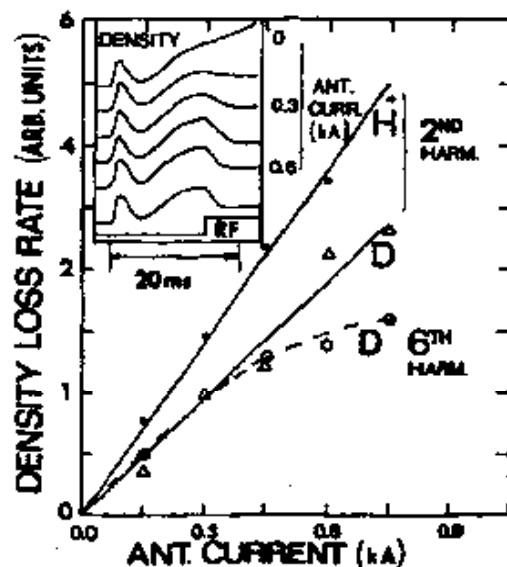


FIG.6. Rate of density loss versus antenna current in H and D plasmas. The insert shows the oscillogram in an H plasma at various antenna currents.

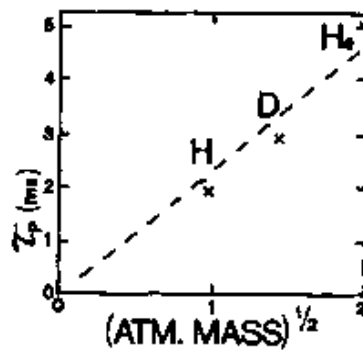


FIG. 7. Global particle containment versus ion mass in H, D and He plasmas under typical experimental conditions.

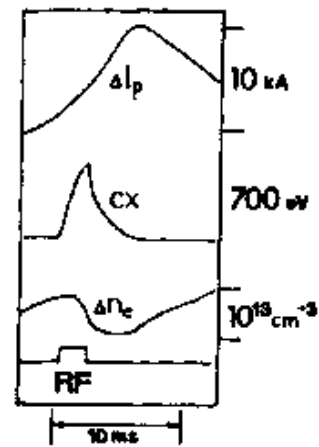


FIG. 8. Oscillograms of current rise and density drop due to a short rf pulse. The density drop in the center is delayed by 2 ms at high densities. The density drop at the edge is prompt (not shown).

When operating in H, D and He plasmas, the particle containment time increases somewhat as the square root of the mass. This is shown in Fig. 7.

Fig. 8 shows the time behavior of the density integrated along a central chord, on an expanded time scale for a short RF pulse. The density drop appears delayed with respect to the RF pulse by 2 msec. At the edge of the plasma, near the antenna, the density drop is prompt, less than 50  $\mu$ sec. This indicates that the center is affected by a diffusion process, not directly by the RF field which quickly (10  $\mu$ sec) builds up at the center. It appears that the edge heating is responsible for the transport, and that the edge temperature varies as the square of the antenna current. Convective transport at the edge may then be driven at a rate proportional to the ion sound velocity, that is, proportional to the square root of the edge temperature over the atomic mass. This density drop may not be observable in devices where the impurity influx cools the plasma edge [6]. In that case the resulting cold plasma may block off the escaping particles, and a density rise may be observed even without a central impurity increase.

## Part B

### MAGNETIC FIELD FLUCTUATIONS IN THE CALTECH RESEARCH TOKAMAK

(M.A. Hedemann, B.S. Levine, R.W. Gould)

Recently there has been great interest in magnetic field fluctuations in tokamaks, since various mechanisms have been proposed [7-10] by which they might explain the observed anomalous electron thermal transport.

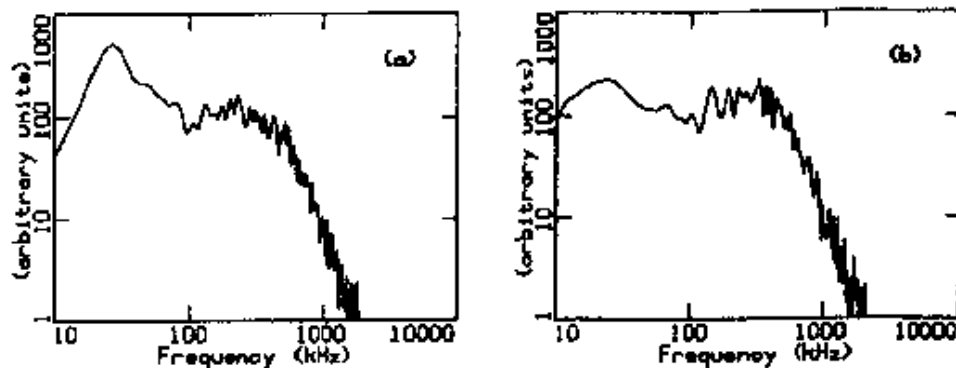


FIG. 9. Spectral density for (a) poloidal magnetic field fluctuations and (b) radial magnetic field fluctuations.

We report experimental results on the characteristics of broadband magnetic field fluctuations observed in the Caltech Research Tokamak ( $R=0.46\text{m}$ ,  $a=0.15\text{m}$ ,  $B_T \sim 5\text{T}$ ,  $I_p \sim 30\text{kA}$ ,  $T_e \sim 100\text{--}200\text{eV}$ ) from magnetic probes inserted into the plasma. Similar measurements have been reported on the Macrotron tokamak [11]. A multi-channel digital data acquisition system with a Nyquist frequency of 2 megahertz (and in some situations to 10 MHz) is employed which permits continuous recording of signals from spatially separated probes which measure various components of the fluctuating field. These signals are archived for spectral, correlation and coherence analyses.

A strong  $m=2$  oscillation ( $f \sim 20\text{kHz}$ ) dominates the first 2 msec of the discharge (the current penetration phase). The amplitude decays rapidly as the electron density falls from a peak value of  $10^{13}\text{cm}^{-3}$  to  $3 \times 10^{12}\text{cm}^{-3}$ . Mode number can be established from the phase of the cross power spectral density of two probes with different poloidal locations.

Later in the discharge, when the electron density has settled to a relatively constant value, the application of these measurement techniques has shown relatively broadband spectra, up to 1 MHz. During this phase, the r.m.s. fluctuation level of both the radial and the poloidal components is 1-5 Gauss ( $\sim 10^{-2} B_p$  or  $\sim 10^{-3} B_T$ ). The r.m.s. fluctuation level of the toroidal component is <20% of this. The fluctuations propagate in the electron diamagnetic drift direction with a phase velocity of  $\sim 10^6\text{cm/sec}$ . The fluctuations are well correlated only for probe separations  $< \sim 5\text{cm}$ . The  $B_p$  spectrum is dominated by low frequencies ( $f \sim 20\text{--}40\text{kHz}$ ), while the  $B_r$  spectrum is flat to  $\sim 300\text{kHz}$ . The spectral density of both  $B_p$  and  $B_r$  decreases monotonically above these frequencies as  $f^{-m}$  with  $m$  varying from a value of 2 to 4 during the shot (Figure 9).

The time development of magnetic fluctuations, their spectra, correlation lengths and coherence have also been studied during density buildup and decay from neutral gas-puffing. During the density rise, an exponentially growing  $m=2$  oscillation

with a growth time of 0.2 msec is observed, which compares well with resistive tearing-mode theory. This mode reaches a saturation amplitude ( $B_p$ ) of a few Gauss. It is highly monochromatic and exhibits a high coherence between probes. During the density decay, a multi-peaked coherent mode structure, which has been identified as the fundamental and (strong) harmonics of the  $m=2$  and the  $m=3$  modes, has been observed. The harmonics are seen to rotate with the appropriate fundamental, and are believed to originate as deformations of  $m=2,3$  magnetic islands. An  $m=7, n=2$  mode ( $f \sim 77$  kHz) is also frequently seen. An  $m=5$  mode ( $f \sim 55$  kHz) is seen occasionally. The maximum achievable density prior to disruptions is found to be consistent with the Murakami limit.

No direct experiments have been done which connect fluctuations with anomalous electron thermal transport. Although much of the energy of the magnetic field fluctuations resides in the low-frequency ( $f < 100$  kHz) portion of the spectrum in what appear to be partially coherent modes, at least 10% ( $\sim 10^{-9} B_T$ ) of the field strength is present in the broadband non-modal portion of the spectrum. This may be enough to provide transport.

### Part C

#### FLUCTUATION MEASUREMENTS ON THE UCLA TOKAMAKS

*(P. Lee, N.C. Luhmann, Jr., A. Mase, W.A. Peebles, A. Smet, S.J. Zweben)*

Low-frequency electron density fluctuations ( $f = 5$  kHz - 1 MHz) in the UCLA Microtor tokamak have been studied using CW far-infrared (FIR) laser scattering and compared with standard probe techniques. The measurements are performed in two regimes: low-density ( $n_e = 2 \times 10^{13}$  cm $^{-3}$ ) and high-density ( $n_e \geq 5 \times 10^{13}$  cm $^{-3}$ ) plasmas. In the latter case, preliminary ICRF heating studies have also been performed and the effects on low-frequency fluctuations are briefly reported.

FIR lasers are ideally suited to the study of collective fluctuations in magnetic fusion plasmas. For FIR lasers the scattering angle is large ( $\theta = 1-40^\circ$  for typical fusion plasma parameters). Therefore, they provide good spatial resolution ( $\Delta x = 1-3$  cm) while simultaneously providing good wavenumber resolution ( $\Delta k \lesssim 3$  cm $^{-1}$ ). Additionally, by varying the source wavelength in the FIR, one can determine the wavenumber spectrum  $S(k)$  over a wide region of  $k$ -space, which is of importance when calculating absolute density fluctuation levels.

For the FIR homodyne scattering measurements discussed here, the output of an optically pumped FIR laser ( $C^{13}H_3F$ ,  $\lambda = 1.222$  mm,  $P = 3-5$  mW or  $CH_3I$ ,  $\lambda = 0.447$  mm,  $P = 10-15$  mW) enters the plasma along a vertical plane where the beam diameter

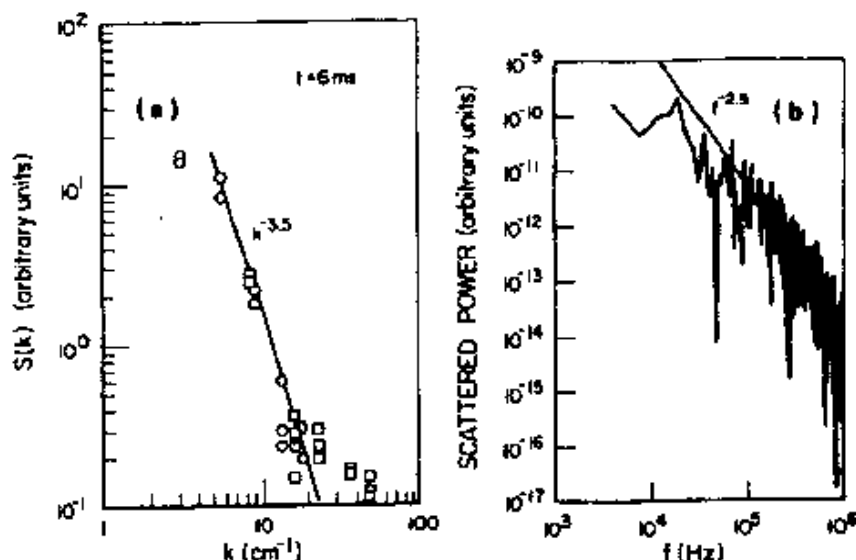


FIG.10. (a) Wavenumber spectrum of scattered 1.222-mm (circles) and 0.477-mm (squares) radiation. (b) Frequency spectrum of scattered 1.222-mm radiation.

is 2.5 cm for  $C^{13}H_3F$  or 1.5 cm for  $CH_3I$ . The scattered light in the same plane as the input beam is collected by a movable mirror which allows the variation of the scattering angle  $\theta$  from  $0^\circ$  to  $20^\circ$ . Thus, the wavevector to be detected is perpendicular to the toroidal field. Near the plasma center the scattering occurs primarily from the  $k_\theta$  component of the fluctuations while at the plasma edge the  $k_r$  contribution dominates.

The I.F. signal is amplified by a series of low-noise amplifiers (1.5 dB N.F.,  $\Delta f = 10$  kHz–10 MHz,  $G = 70$ –90 dB) and fed either directly into a high speed digitizer for waveform analysis, or into a crystal detector in order to study the time evolution of the frequency-integrated signal.

Detailed experiments were performed in the low-density regime [12] and the following features were typically observed.

(1) As shown in Fig. 10, the density fluctuations exhibit a power law fall-off  $\omega^{-2.5}$  between 100 kHz and 500 kHz and  $k^{-3.5}$  for  $6 \text{ cm}^{-1} \leq k_1 \leq 20 \text{ cm}^{-1}$  ( $0.6 \leq k_1 \rho_1 \leq 2$ ). A large enhancement of the very low frequency components ( $f < 20$  kHz) is observed. The spectrum of the density fluctuations detected by Langmuir probes was also found to scale as  $(\tilde{n})^2 \propto \omega^{-2.5}$  for  $f > 100$  kHz.

(2) This spectral shape is independent of radial position  $r$ , which means that an isotropic turbulence spectrum is formed in a two-dimensional plane.

(3) Total density fluctuations obtained by integration of  $S(\underline{k}, \omega)$  over  $\omega$  and  $\underline{k}$  are found to be peaked at the plasma edge, yielding  $\tilde{n}/n_0 = 1.5\%$ .

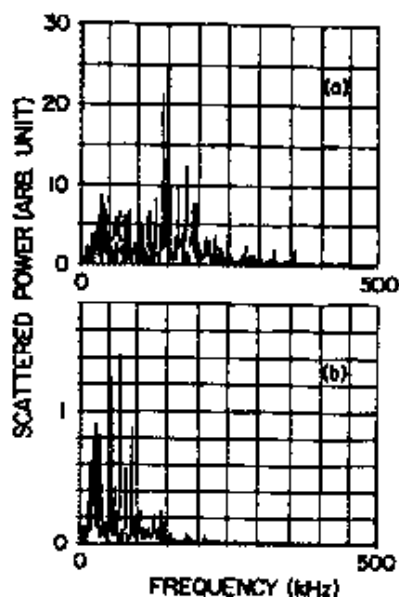


FIG.11. Frequency spectrum of scattered 1.222-mm radiation at two radial positions: (a)  $r = 0$  cm; (b)  $r = 10$  cm.

Preliminary results have been obtained in the high-density plasma with and without ICRF heating. Figure 11 shows the frequency spectra at two different radial positions. It is seen that the high-frequency components are enhanced at small values of  $r$  (i.e.  $k_{\theta} \gg k_{r}$ ).

Linear theory predicts that the waves will lie in the drift wave frequency region with  $\omega = \omega^* = k_{\theta} v_d^*$ , where  $v_d^*$  is the electron diamagnetic drift velocity,  $v_d^* = 2-4 \times 10^5$  cm/sec. For  $k_{\theta} = 3.6$  cm $^{-1}$  ( $r=0$ ) we obtain  $\omega^*/2\pi = 100-200$  kHz, which is consistent with observed peak. These results are in contrast to the low-density case ( $n_e \leq 2 \times 10^{13}$  cm $^{-3}$ ) where the very low frequency components ( $f \leq 20$  kHz) dominate at all radial positions.

Recently, FIR scattering has been performed during ICRF heating although the antenna structure had not yet been optimized. The wavenumber spectra were compared with and without ICRH as shown in Fig. 12. The power law fall-off in wavenumber spectra is  $k^{-3.5 \pm 0.5}$  without rf which is the same as the low-density plasma case while  $k^{-3.1 \pm 0.4}$  with rf. Typical normalized density fluctuation levels of  $\sim 4\%$  are observed in both cases.

The energy confinement time calculated from the measured plasma parameters is  $\approx 1$  msec for the low-density and  $\approx 5$  msec for the high-density case. These allow estimates of the global heat diffusion coefficient  $D_E = a^2/4\tau_E \sim 3 \times 10^4$  cm $^2$ /sec and  $6 \times 10^3$  cm $^2$ /sec, respectively. This can be compared with the enhanced diffusion expected from low-frequency microturbulence. Cheng and Okuda [13], using computer simulations, have shown that convective cells can be excited nonlinearly by drift instabilities. These cells have different frequency spectra from that of the drift waves with more spectral weight at small  $\omega$ , in qualitative agreement with the data shown in Fig. 10. In addition, they give rise to an anomalous diffusion coefficient  $D = (cT_e \rho_i) eBL_n$  which yields  $(1-4) \times 10^4$  cm $^2$ /sec for our experimental parameters, which is in good agreement with the energy confinement time for the low-density plasma.

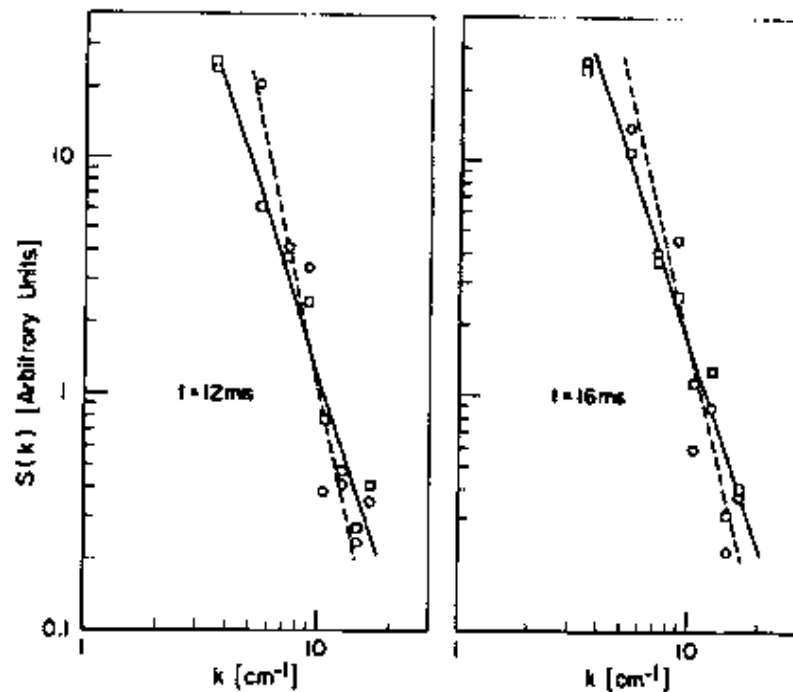


FIG.12. Wavenumber spectrum of scattered 1.222-mm radiation at two times in the tokamak discharge with (squares) and without (circles) ICRF heating.

From the usual quasilinear procedure, the cross-field diffusion coefficient due to the electrostatic drift wave fluctuations is estimated as  $D = \gamma L_n^2 |\tilde{n}/n_0|^2$  where  $\gamma$  is the growth rate of the linear unstable wave. If we assume that  $\gamma^{-1}$  is roughly given by the measured auto-correlation time of the fluctuations ( $\sim 4 \mu\text{sec}$ ), we find  $D = 10^3 \text{ cm}^2/\text{sec}$  for  $\tilde{n}/n_0 = 1.5\%$  and  $7 \times 10^3 \text{ cm}^2/\text{sec}$  for  $\tilde{n}/n_0 = 4\%$ . The latter value is in good agreement with the energy confinement of the high-density plasma.

In conclusion, we have observed for the first time the power spectra of density fluctuations in the Microtor tokamak by using FIR laser scattering. These fluctuations may be identified as collisionless drift waves and nonlinearly excited convective cells. It is shown that these fluctuations may be one of the main causes of anomalous transport, which is much larger than that predicted by the neoclassical theory.

## REFERENCES

- [1] GONDHALEKAR, A., et al., in *Plasma Physics and Controlled Nuclear Fusion Research 1978* (Proc. 7th Int. Conf. Innsbruck, 1978) Vol.1, IAEA, Vienna (1979) 199.
- [2] TFR GROUP, in *Proc. 4th Kiev Int. Conf. in Plasma Theory and 4th Int. Congress on Waves and Instabilities in Plasmas*, Nagoya, 1980.
- [3] PERKINS, F.W., *Nucl. Fusion* 17 (1977) 1197.

- [4] ADAM, J., et al., in *Plasma Physics and Controlled Nuclear Fusion Research 1974* (Proc. 5th Int. Conf. Tokyo, 1974) Vol.1, IAEA, Vienna (1975) 65.
- [5] GOLOVATO, S.N., SHOHET, J.L., *Phys. Fluids* 21 (1978) 1421.
- [6] SUCKEWER, S., HAWRYLUK, R.J., *Phys. Rev. Lett.* 40 (1978) 1649.
- [7] CALLEN, J.D., *Phys. Rev. Lett.* 39 (1977) 1540.
- [8] RECHESTER, A.B., ROSENBLUTH, M.N., *Phys. Rev. Lett.* 40 (1978) 38.
- [9] OHKAWA, T., *General Atomic Rep. A14433* (May 1977).
- [10] DRAKE, J.F., GLADD, N.T., LIU, C.S., CHANG, C.L., *Phys. Rev. Lett.* 44 (1980) 994.
- [11] ZWEBEN, S.J., MENYUK, C.R., TAYLOR, R.J., *Phys. Rev. Lett.* 42 (1979) 1270.
- [12] SEMET, A., MASE, A., PEEBLES, W.A., LUHMANN, N.C., Jr., ZWEBEN, S., submitted to *Phys. Rev. Lett.*
- [13] CHENG, C.Z., OKUDA, H., *Nucl. Fusion* 18 (1978) 587.

## DISCUSSION

F. WAELBROECK: You have shown that ICRF heating increases the temperature but causes a density decrease for deuterium plasmas in Macrotor. Is the net effect an increase in the total plasma energy and, if so, what is its magnitude? Increasing the plasma energy tends to shift the plasma position radially outwards and enhances the plasma-antenna contact. What provisions, such as feedback control, exist on Macrotor to limit this outward displacement and prevent resultant particle losses, which are expected to be much larger for D than for He because of the different recycling properties on the metal surface?

R.J. TAYLOR: The plasma energy increases from  $\beta(0) = 1\%$  to  $\beta(0) = 3\%$ . The radial shift is accommodated by anticipating it with programming. There are, however, also some problems with feedback systems, so we have not used them. The difference between the recycling of D and He is intrinsically so large that plasma motion is not observed to be a significant factor in the results.

P.E. JACQUINOT: Did you study the effect of minority concentration on heating and pump-out?

R.J. TAYLOR: Yes. The minority contribution to heating is significant; the effect on pump-out is not. However, we have observed some minority transport in the axial direction at the cyclotron layer by using Faraday-cup detectors.

P. VANDENPLAS (*Chairman*): Did you make a systematic investigation of the damping mechanism and under what conditions do you have maximum power absorption?

R.J. TAYLOR: It is still difficult to show maximum power absorption by direct dialling conditions owing to the complexity of the operating regimes. However, on the basis of results over the last two years, the two-ion regime looks more efficient than the H-second harmonic by a factor of two. This conclusion may be altered in the future as a result of changes in the excited power spectrum produced by new antennae.

T. TAMANO: Can you be certain that the density change is due to the presence of RF fields rather than to a change in local temperature?

R.J. TAYLOR: Both factors may be important, the major effect possibly coming from the edge temperature, which is not cooled by impurities in our case.

R. ITATANI: I would like to comment on the importance of mode selection for ICRF heating. Linearly polarized RF fields generate convective plasma motions because the ponderomotive force enhances the plasma losses. On the other hand, rotating RF fields do not give rise to convection. These conclusions have been confirmed experimentally on both a small tokamak and a linear plasma.